

# Point-wise Convolutional Neural Network

Binh-Son Hua

Minh-Khoi Tran

Sai-Kit Yeung

Singapore University of Technology and Design

## Abstract

Deep learning with 3D data such as reconstructed point clouds and CAD models has received great research interests recently. However, the capability of using point clouds with convolutional neural network has been so far not fully explored. In this technical report, we present a convolutional neural network for semantic segmentation and object recognition with 3D point clouds. At the core of our network is point-wise convolution, a new convolution operator that can be applied at each point of a point cloud. Our fully convolutional network design, while being surprisingly simple to implement, can yield competitive accuracy in both semantic segmentation and object recognition task.

## 1. Introduction

Deep learning with 3D data has received great research interests recently, which leads to noticeable advances in typical applications including scene understanding, shape completion, and shape matching. Among these, scene understanding is considered as one of the most important tasks for robots and drones as it can assist exploratory scene navigations. Tasks such as semantic scene segmentation and object recognition are often performed to predict contextual information about objects for both indoor and outdoor scenes.

Unfortunately, deep learning in 3D was deemed difficult due to the fact that there are several ways to represent 3D data such as volumes, point clouds, or multi-view images. Volume representation is a true 3D representation and straightforward to implement but often requires a large amount of memory for data storage. By contrast, multi-view representation is not a true 3D representation but shows promising prediction accuracy as existing pre-trained weights from 2D networks can be utilized. Among such representations, point clouds have been the most flexible as they are compact and could be exported from a wide range of CAD modelling and 3D reconstruction software. However, the capability of using point clouds with neural

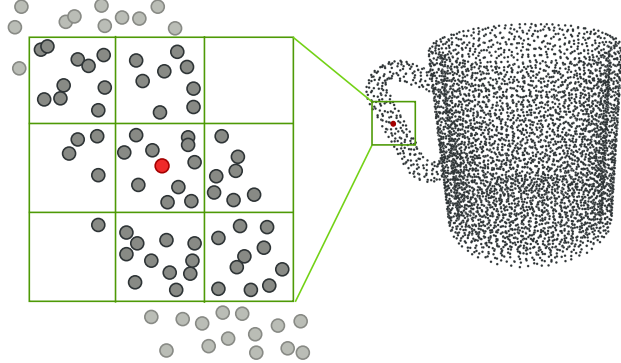


Figure 1: Point-wise convolution. We define a new convolution operator for point cloud input. For each point, nearest neighbors are queried on the fly and binned into kernel cells before convolving with kernel weights. By stacking point-wise convolution operators together, we can build fully convolutional neural networks for scene segmentation and object recognition for point clouds.

network has been so far not fully explored.

In this technical report, we present a convolutional neural network for semantic segmentation and object recognition with 3D point clouds. At the core of our network is a new convolution operator, called *point-wise convolution*, which can be applied at each point in a point cloud to learn point-wise features. This leads to surprisingly simple and fully convolutional network designs for scene segmentation and object recognition. Our experiments show that point-wise convolution can yield competitive accuracy to previous techniques while being much simpler to implement. In summary, our contributions are:

- A point-wise convolution operator that can output features at each point in a point cloud;
- Two point-wise convolutional neural networks for semantic scene segmentation and object recognition.

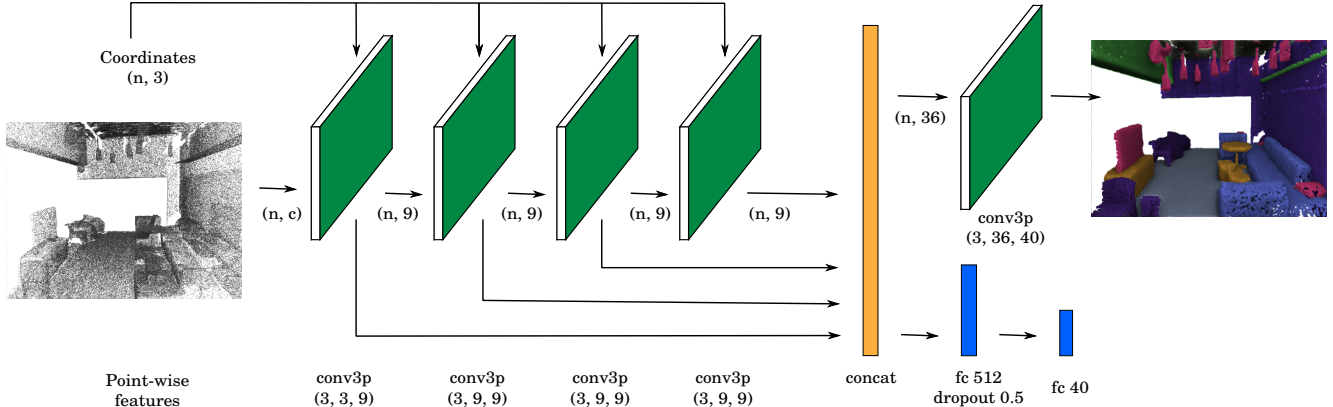


Figure 2: Point-wise convolutional neural network. The input point cloud is fed into each convolution operator (conv3p), and all outputs are concatenated before being fed to a a final convolution layer for dense semantic segmentation, or to fully connected layers for object recognition. In this figure, we assume point cloud with  $n$  points and  $c$  attributes (colors, normals, coordinates, etc.). We use 9 output channels for each convolution operator before concatenation.

## 2. Related Works

Recently, there has been a great number of works about deep learning with 3D data. Let us focus on those for scene understanding tasks such as semantic segmentation and object recognition.

### 2.1. Shape descriptors

Hand-crafted shape descriptors were widely used in computer vision and graphics applications before the era of deep learning. For example, 3D shapes can be projected into 2D images and represented by a set of 2D descriptors on such images. Shapes can then be represented as histograms or bag-of-feature models which can be constructed from surface normals and curvatures [11]. 3D shapes can also be represented by their inherent statistical properties, such as distance distribution [24] and harmonic descriptors [14]. Heat kernel signatures extract shape descriptions by simulating an heat diffusion process on 3D shapes [34]. The Light Field Descriptor (LFD) is another popular descriptor useful in the shape classification tasks. It extracts geometric and Fourier descriptors from object silhouettes rendered from several different viewpoints [4]. Despite their long history and being widely used, hand-crafted 3D shape descriptors do not generalize well across different domains.

### 2.2. Object recognition

Convolutional neural networks (CNNs) [17] has been successfully applied in various areas of computer vision and artificial intelligence. Recently, significant achievements have been reached in understanding images through learning features by CNNs. Large RGB image datasets like ImageNet [6] can be used in training a CNN, which is in turn able to learn general purpose image descriptors from such

datasets. Image descriptors generated by CNNs are proved to greatly outperform other hand-crafted features for various tasks, including object detection [8], scene recognition [7], texture recognition [29], [5] and classification [9].

Recently, several approaches to using 3D convolutional networks to extract shape descriptor have been proposed, ranging from voxel-based representation [37, 19] panorama [30], feature pooling from 2D projections from multiple viewpoints [33, 26], to point set [26]. Among these, Qi et al. [25]’s PointNet is one of the first network architecture that can handle point cloud data. PointNet is robust as it can take point clouds of arbitrary orders as input. Subsequently, Kd-Networks [16] leverage a kd-tree structure to build a computational graph for object recognition. However, networks based on PointNet have to rely on a prefix network to learn a symmetric function to turn a point cloud into a set before performing their further learning and predictions. In this work, we propose point-wise convolution network, and show that it is possible to perform scene understanding tasks such as semantic segmentation and object recognition on *ordered* point clouds. The network design can also be fully convolutional. This is an important feature in order to stack many layers together to design very deep networks.

### 2.3. Semantic segmentation

There are considerably great numbers of related works in semantic segmentation. Since the introduction of the NYUv2 dataset from Silberman *et al.* [31], there has been a spark the direction of RGBD semantic segmentation. The work from Long *et al.* [18] showed how to adopt a conventional classification network for the semantic segmentation problem. Since then, different techniques have been proposed to further improve the segmentation results. Some

notable examples are SegNet [3] employing an encoder-decoder architecture, or dilation filter from Yu [38].

In the 3D domain, interactive techniques [36, 35] relied on user strokes to propagate segmentation. McCormac et al. [20] explored transferring semantic segmentation from 2D predictions to the 3D domain. An advantage of such methods is that they can produce high-resolution segmentation. However, none of the predictions can be performed directly on the 3D domain.

SSCNet [32] applied convolutional neural network to a 3D volume representation to classify each voxel in the scene. This could be flexible as real-time scene reconstruction techniques such as KinectFusion [22] and voxel hashing [23] are often based on volumes. PointNet [25] can also be used for semantic segmentation with minor modifications from their object recognition network. In this paper, we demonstrate a fully convolutional neural network for 3D point cloud segmentation.

### 3. Point-wise Convolution

Before presenting point-wise convolution, we briefly revise a few possibilities to represent 3D data for neural network. The most straightforward approach is perhaps to employ volumetric representation. For example, VoxNet [19] represents each object by a volume up to  $64 \times 64 \times 64$  resolution. This is natural because almost existing network architecture for image applications can be adopted. However, a significant drawback is that volumetric representation requires a large amount of memory while the number of non-zero values in a volume only accounts for a very small percentage. This could be addressed by a sparse representation [28].

A second possibility is to use point clouds. This is a direct representation as point cloud is often the output of many applications such as RGB-D reconstruction and CAD modeling. However, mapping point cloud to neural network is not natural because traditional convolution operators are only designed for grid and volumes. PointNet [25] implements point feature learning by fully connected layers.

The previous limitations motivate us to design fully convolutional networks for point clouds. The basic building block of our architecture is a convolution operator applied at each point in a point set, which we term *point-wise convolution* operator. This operator works as follows.

**Convolution.** A convolution kernel is centered at each point. Neighbor points within the kernel support can contribute to the center point. Each kernel has a size or radius value, which can be adjusted to account for different number of neighbor points in each convolution layer. Figure 1 shows a diagram that demonstrates this idea.

Formally, point-wise convolution can be written as

$$x_i^\ell = \sum_k w_k \frac{1}{|\Omega_i(k)|} \sum_{p_j \in \Omega_i(k)} x_j^{\ell-1}, \quad (1)$$

where  $k$  iterates over all sub-domains in the kernel support;  $\Omega_i(k)$  is the  $k$ -th sub-domain of the kernel centered at point  $i$ ;  $p_i$  is the coordinate of point  $i$ ;  $|\cdot|$  counts all points within the sub-domain;  $w_k$  is the kernel weight at the  $k$ -th sub-domain,  $x_i$  and  $x_j$  the value at point  $i$  and  $j$ , and  $\ell - 1$  and  $\ell$  the index of the input and output layer.

**Gradient backpropagation.** Suppose that  $L$  is the loss function. The gradient with respect to input could be defined as

$$\frac{\partial L}{\partial x_j^{\ell-1}} = \sum_{i \in \Omega_j} \frac{\partial L}{\partial x_i^\ell} \frac{\partial x_i^\ell}{\partial x_j^{\ell-1}} \quad (2)$$

where we iterate over all neighbor points  $i$  of a given point  $j$ . In the chain rule,  $\partial L / \partial x_i^\ell$  is the gradient up to layer  $\ell$ , which is known during back propagation. The derivative  $\partial x_i^\ell / \partial x_j^{\ell-1}$  could be written as

$$\frac{\partial x_i^\ell}{\partial x_j^{\ell-1}} = \sum_k w_k \frac{1}{|\Omega_i(k)|} \sum_{p_j \in \Omega_i(k)} 1 \quad (3)$$

Similarly, the gradient with respect to kernel weights could be defined by iterating over all points  $i$ :

$$\frac{\partial L}{\partial w_k} = \sum_i \frac{\partial L}{\partial x_i^\ell} \frac{\partial x_i^\ell}{\partial w_k} \quad (4)$$

where

$$\frac{\partial x_i^\ell}{\partial w_k} = \frac{1}{|\Omega_i(k)|} \sum_{p_j \in \Omega_i(k)} x_j^{\ell-1} \quad (5)$$

Note that the above formula does not assume a specific shape for convolution kernel. Here we simply use a uniform grid kernel. In conjunction with a grid acceleration structure, the convolution operator can be efficiently implemented on both CPU and GPU. In this paper, we use convolution kernels of size  $3 \times 3 \times 3$ . All points within each kernel cell have the same weights.

Unlike convolution in volumes, in our design, we do not use pooling. There are some advantages of doing so. First, it is no longer required to deal with point cloud downsampling and upsampling, which is not straightforward when the point attributes become high dimensional when the point cloud is processed in the network. Second, by keeping the point cloud unchanged in the entire network, acceleration structures for neighborhood lookup only need to be built once. This significantly speeds up computation and simplifies network design.

**Point order.** A notable difference between our design and PointNet [25] is how points are ordered before being fed to the network. In PointNet, point cloud is orderless, and the training process of PointNet learns a symmetric function to turn an ordered point cloud into orderless. However, we argue that this is not necessary. In our method, we input points sorted in a specific order, e.g., XYZ or Morton curve [21], to the network and can still achieve competitive performance in object recognition and semantic segmentation task.

**À-trous convolution.** The original point-wise convolution can be easily extended to à-trous convolution by including a stride parameter that determines the gaps between kernel cells. The benefit of point-wise à-trous convolution is that it is possible to extend the kernel size, and hence the perceptive field, without actually processing too many points in the convolution. This yields significant speed up without sacrificing accuracy as to be demonstrated in our experiments.

**Point attributes.** For easy housekeeping in the implementation of our convolution operator, we separately store point coordinates and other point attributes such as colors, normals, or other high-dimensional features output from preceding convolutional layers. Point coordinates can be passed to any layer despite the layer depth so that they can be used for neighbor queries to determine which points can participate in the convolution at a particular point. Point attributes can then be retrieved accordingly.

## 4. Point-wise Convolutional Neural Network

Point-wise convolution can now be applied to build classification networks. The network design is shown in Figure 2. Here we follow the design of VoxNet [19]. A point cloud with XYZ coordinates is used as input to four point-wise convolution layers with gradual increasing kernel radius. In all layers, we keep the kernel dimensions to  $3 \times 3 \times 3$ . When the kernel radius is increased, more points fall into the same kernel cell, allowing the perceptive field of the kernel to widen to a larger neighborhood. To output object categories, the all features from all layers are concatenated and passed through two fully connected layers with size 512 and the number of object categories, respectively. Between the last two fully connected layers, dropout of rate 0.5 is applied to regularize the learning.

To normalize the network parameters, we employ self-normalizing activation function (SELU) [15]. The end effect of SELU is equivalent to batch normalization which allows more effective regularization of the training. Note that we experimented with traditional ReLUs and found that training converges more slowly than training with SELU.

We can then adopt this classification network design for

semantic segmentation. We keep the all convolutional layers from the object recognition network, and remove the last two fully connected layers. We then add a new point-wise convolutional layer to output the confidence of each category at each point, resulting in a fully convolutional neural network for semantic segmentation for 3D point clouds.

We implement point-wise convolution on both the CPU and the GPU in Tensorflow [1]. The input point cloud is passed into the operator together with other point cloud attributes. We experiment with point clouds of size 2048 in object recognition, and 4096 in semantic segmentation. Since the number of points is low, we only use a grid acceleration structure on the CPU implementation for neighbor queries. On the GPU, we simply implemented a brute-force search as we found that generating a grid or other hierarchical data structure at each convolution does not accelerate the computation due to small point clouds.

We train the network from scratch with momentum gradient optimization. The momentum value set to 0.9, learning rate 0.001 with exponential decay 0.96. Unless explicitly mentioned, the training parameters are also kept unchanged for all other training tasks such as scene segmentation.

## 5. Evaluations

**Semantic segmentation.** We evaluate our point-wise convolutional neural network with semantic scene segmentation and object recognition. For scene segmentation, we first experiment with the S3DIS dataset [2], which has 13 categories of indoor scene objects. Each point has 9 attributes: XYZ coordinates, RGB color, and normalized coordinates w.r.t. the room space it belongs to. To perform segmentation of a scene, each squared-meter block of the scene (measured on the floor), sampled to 4096 points, are fed into the network. The predictions of all blocks are then assembled to obtain the prediction of the entire scene.

We report per-point accuracy of the semantic segmentation. Our network is able to produce comparable accuracy to PointNet [25], with the accuracy of 81.5%. PointNet was originally reported to achieve 78.1% in [25]. Table 1 reports per-class accuracy. Figure 3 shows visualization of predictions and ground truths of the scenes in the evaluation dataset.

To further test semantic segmentation with more categories and more complex indoor scenes, we annotate 76 scenes from the SceneNN dataset [12] with 40 categories defined by the NYU v2 dataset [31]. Scenes in this dataset appear to be more cluttered, which poses great challenges to semantic segmentation. We use 56 scenes for training, and 20 scenes for evaluation. In each scene, a  $2 \times 2$  sqm. window with stride 0.2 meter and height 2 meters is used to scan the floor area, resulting in approximately 30K scene blocks for training and 15K blocks for testing. Each block

Network	ceiling	floor	wall	column
PointNet [25]	98.3	98.8	83.3	63.4
Ours	97.4	99.1	89.1	56.2
door	table	chair	sofa	clutter
PointNet [25]	84.6	70.3	66.0	56.7
Ours	62.9	73.7	68.4	54.6
				65.2

Table 1: Per-class accuracy of semantic segmentation on S3DIS dataset [2].

is sampled to 4096 points.

The visualization of the predictions and ground truth are shown in Figure 4. It can be seen that structures like wall and floor have very good accuracy, and small objects are moderately well segmented. A notable issue is noise due to prediction inconsistency in the overlap regions of the blocks. This could be addressed by a conditional random field and would be an interesting future work.

Table 2 reports the accuracy of a few common categories. Note that not all NYU categories are available. While structures and chairs are quite accurate, table and desk are often ambiguous, resulting in lower accuracy for both classes.

Network	wall	floor	chair	table	desk
Ours	93.8	88.6	58.6	23.5	29.5

Table 2: Per-class accuracy of semantic segmentation on SceneNN dataset [12].

**Object recognition.** We evaluate object recognition with two datasets, ModelNet40 [37] and ObjectNN [13]. ModelNet40 is a CAD model dataset of 40 categories which has served as a standard benchmark for object recognition in the recent years. On the other hand, ObjectNN is an object dataset from RGB-D scene reconstruction mixed with CAD models for studying 3D object retrieval. Objects in ObjectNN is particularly difficult to classify because they are reconstructed from noisy RGB-D data and often has missing parts.

For object recognition, our point attributes are simple XYZ coordinates. In fact, we also trained the network with point attributes set to one, making the convolution equivalent to density estimation, and found no significant change in accuracy. Our results on ModelNet40 are shown in Table 3. As can be seen, our network performs comparably to state-of-the-art methods. Note that compared to VoxNet [19], our point cloud and convolutional network is a more compact. Our network is also significantly simpler in design compared to PointNet [25] and PointNet++ [27] while being close to their accuracy.



Figure 3: Visualization of our semantic segmentation results using point-wise convolutional network and ground truth scenes from S3DIS dataset [2].

The results on ObjectNN are shown in Table 4. In this dataset, again our method performs comparably to PointNet, but overall both methods are less effective due to the

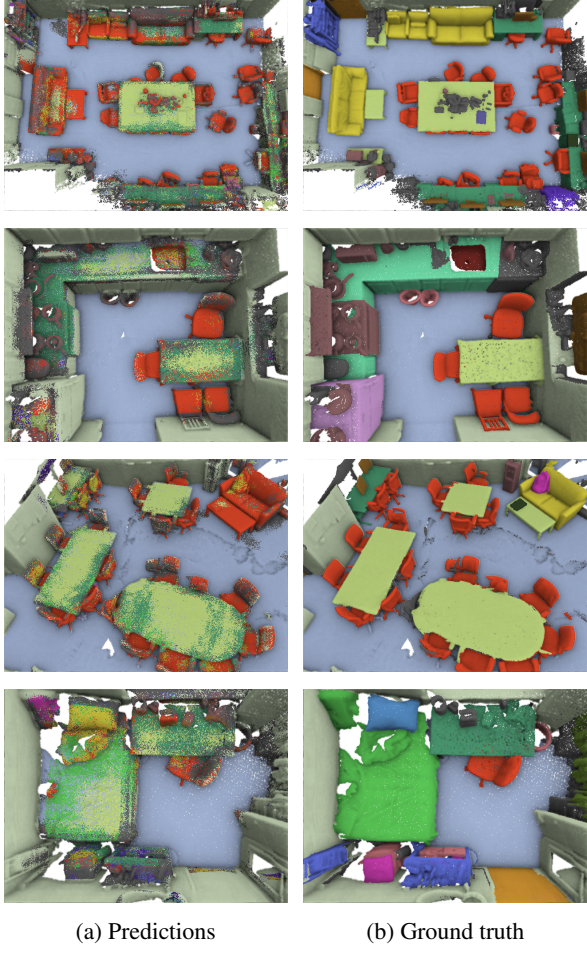


Figure 4: Semantic segmentation on the SceneNN dataset.

Network	Accuracy (per class)	Accuracy
VoxNet [19]	83	-
MO-SubvolumeSup [26]	86	89.2
PointNet [25]	86.2	89.2
PointNet++ [27]	-	90.7
Ours	81.4	86.1

Table 3: Comparison of performance of network architectures using 3D object representations on the ModelNet40 dataset [37].

ambiguity in learning features from both CAD models and RGB-D objects.

Table 9 and Table 10 further provide per-class accuracy on the ModelNet40 and the ObjectNN dataset, respectively.

**Convergence.** Figure 5 shows a plot of the training and test accuracy of our networks over time. The graph shows

Network	Accuracy (per class)	Accuracy
PointNet [25]	57.1	65.6
Ours	57.1	65.1

Table 4: Comparison of object recognition accuracy on the ObjectNN dataset [13].

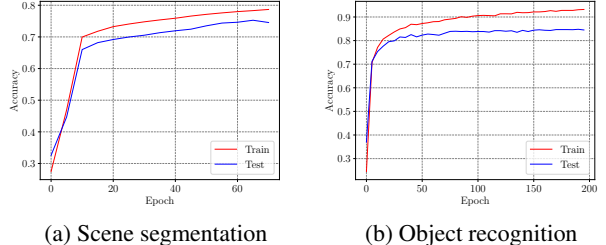


Figure 5: Train and test accuracy over time.

that our point-wise convolutional neural network can be trained effectively.

**Ablation experiments.** Here we analyze the effectiveness of point-wise convolution. We first start with a basic 4-layer model as in Figure 2. The accuracy improvement when more features are added are presented in Table 5. As can be seen, feature concatenation, à-trous convolution, SELU activation, and dropout each contributes a small improvement to the final result.

Base	Concat.	À-trous	SELU	Dropout	Accuracy
✓					78.6
✓	✓				78.0
✓		✓			75.0
✓	✓	✓			82.5
✓			✓		81.7
✓	✓		✓		81.9
✓	✓		✓	✓	85.2
✓	✓	✓	✓	✓	86.1

Table 5: Ablation experiment. Accuracy improvement is achieved when point-wise convolution is combined with feature concatenation (Concat.), à-trous convolution, self-normalization activation function (SELU), and dropout.

**Point order.** In object recognition, the order of the input points determine the orders of the features in the fully connected layers. As long as this layer has an order, it is sufficient to discriminate their features and predict the categories. We experiment with different orders of the input

Order	Accuracy
ZYX	86.1
Morton curve	86.0

Table 6: Object recognition with different ways of ordering the input point cloud.

point set and report the results in Table 6. We found that point orders sorted by space filling curve techniques such as Morton curve [21] yields comparable accuracy, which means that it is sufficient to just follow an order, but not a particular one. However, a benefit is that space filling curves organize points such that nearby points in space are stored close to each other in memory, allowing more memory coherence.

**Neighborhood radius.** So far we have been setting the radius for neighbor query as constant in each convolution layer. In our experience, this works well for both tasks. We also explore the capability of adaptive radius using k-nearest neighbors. The modification for the convolution operator is as follows.

At each point, a k-nearest neighbor is performed, and the query radius is set to the distance to the furthest neighbor. This radius is used each time neighbor points have to be queried for convolution. To compute gradients for back-propagation for this operator, it is worth noting that in this case, neighbor lookup is no longer symmetric. Therefore, at a point  $j$ , it is required to look up all points  $i$  such that point  $i$  can contribute to point  $j$  in the forward convolution.

We compare the performance of the k-nearest neighbor and the fixed radius convolution for object recognition task. The result is shown in Table 7. In general, we found no significant difference in terms of accuracy.

Neighbor query	Accuracy
Fixed-size radius	86.1
K-nearest neighbor	85.7

Table 7: Object recognition with convolution using neighbor queries with adaptive radius.

**Deeper networks** Finally, we study the capability of learning with deeper networks using point-wise convolution. From the basic model, we increase the number of layers from 4 to 8 and 16, and then retrain from scratch. The performance are reported in Table 8 below. Generally, it takes longer to train networks with 8 and 16 layers, resulting in slightly slower accuracy. Experimenting the training

Network	Accuracy
4 layers	86.1
8 layers	82.1
16 layers	82.6

Table 8: Deep point-wise convolutional neural network. We compare object recognition performance with 4-, 8-, and 16-layer architecture.

with residual learning [10] would be an interesting future work.

There are some limitations in the current point-wise convolution. Points in the same filter cell has the same convolution weights, which limits the discrimination of points within a cell. A possible solution to investigate is to increase the kernel resolution.

## 6. Conclusion

In this paper, we proposed point-wise convolution for building neural networks for scene understanding with point cloud data. We show that using ordered point cloud in a fully convolutional manner is possible. Our convolution layer is robust and offer competitive accuracy while being simple to implement, allowing us to create effective and simple neural networks for learning local features of point clouds. The resulting features extracted from the network are shown to be robust for tasks such as scene segmentation and object recognition.

There are several research avenues to be further explored. For example, can the filter size be optimized to adapt to input data rather than having to be tuned to work with different point cloud density? Also, it is interesting to explore how to increase the perceptive field and incorporate global features to the point cloud with point-wise convolution to further boost the performance of the networks.

## A. Layer Visualization

Intuitively, point-wise convolution works by summarizing local spatial point distributions to build feature vectors for each point in a point cloud. As shown in per-class accuracy tables, local features work the most effectively in classifying structures such as ceiling, floor, or walls and common furniture such as tables and chairs. In our observation, it is quite challenging to differentiate between tables (for dining) and desks (for study and work).

We visualize the filters of the first four layers in the object recognition network in Figure 6. Here we display each  $3 \times 3 \times 3$  filter on a row in the visualization. The number of rows is equal to the product of the total number of input and output channels of each filter (27 for the first layer, and 81 for the subsequent layers).

Network	airplane	bathtub	bed	bench	bookshelf	bottle	bowl	car	chair	cone
PointNet [25]	100	80.0	94.0	75.0	93.0	94.0	100.0	97.9	96.0	100.9
Ours	100	82.0	93.0	68.4	91.8	93.9	95.0	95.6	96.0	80.0
	cup	curtain	desk	door	dresser	flower pot	glass box	guitar	keyboard	lamp
PointNet [25]	70.0	90.0	79.0	95.0	65.1	30.0	94.0	100.0	100.0	90.0
Ours	60.0	80.0	76.7	75.0	67.4	10.0	80.8	98.0	100.0	83.3
	laptop	mantel	monitor	night stand	person	piano	plant	radio	range hood	sink
PointNet [25]	100.0	96.0	95.0	82.6	85.0	88.8	73.0	70.0	91.0	80.0
Ours	95.0	93.9	92.9	70.2	89.5	84.5	78.8	65.0	88.9	65.0
	sofa	stairs	stool	table	tent	toilet	tv stand	vase	wardrobe	xbox
PointNet [25]	96.0	85.0	90.0	88.0	95.0	99.0	87.0	78.8	60.0	70.0
Ours	96.0	80.0	83.3	90.9	90.0	94.9	84.5	81.3	30.0	75.0

Table 9: Per-class accuracy of object recognition on the ModelNet40 dataset. Average: PointNet: 86.3. Ours 81.4.

Network	chair	display	desk	book	storage	box	table	bin	bag	keyboard
PointNet [25]	84.2	85.4	56.7	30.1	62.5	23.8	80.0	75.0	47.4	82.4
Ours	83.1	85.4	70.0	57.7	45.8	23.8	60.0	65.0	36.8	88.2
	sofa	bookshelf	pillow	machine	pc case	light	oven	cup	printer	bed
PointNet [25]	76.5	23.1	84.6	18.2	36.4	77.8	60.0	37.5	50.0	28.6
Ours	88.2	38.5	76.9	18.2	54.5	88.9	30.0	75.0	12.5	42.9

Table 10: Per-class accuracy of object recognition on the ObjectNN dataset. Average: PointNet: 56.0. Ours: 57.1.

In the visualization, blue and red represent positive and negative values, respectively. White represents zero. This shows that the filters in the network are relatively sparse and smooth. We also observed that positive and negative values dominate the filters interchangeably in each layer.

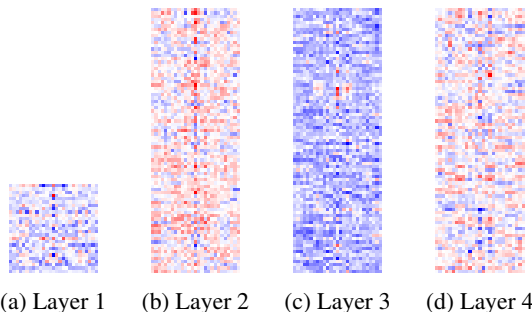


Figure 6: Visualization of the filters in point-wise convolution network for object recognition.

## References

- [1] M. Abadi, A. Agarwal, P. Barham, E. Brevdo, Z. Chen, C. Citro, G. S. Corrado, A. Davis, J. Dean, M. Devin, S. Ghemawat, I. Goodfellow, A. Harp, G. Irving, M. Isard, Y. Jia, R. Jozefowicz, L. Kaiser, M. Kudlur, J. Levenberg, D. Mané, R. Monga, S. Moore, D. Murray, C. Olah, M. Schuster, J. Shlens, B. Steiner, I. Sutskever, K. Talwar, P. Tucker, V. Vanhoucke, V. Vasudevan, F. Viégas, O. Vinyals, P. Warden, M. Wattenberg, M. Wicke, Y. Yu, and X. Zheng. TensorFlow: Large-scale machine learning on heterogeneous systems, 2015. Software available from tensorflow.org. [4](#)
- [2] I. Armeni, O. Sener, A. R. Zamir, H. Jiang, I. Brilakis, M. Fischer, and S. Savarese. 3d semantic parsing of large-scale indoor spaces. In *Proceedings of the IEEE International Conference on Computer Vision and Pattern Recognition*, 2016. [4, 5](#)
- [3] V. Badrinarayanan, A. Kendall, and R. Cipolla. Segnet: A deep convolutional encoder-decoder architecture for image segmentation. *arXiv preprint arXiv:1511.00561*, 2015. [3](#)
- [4] D.-Y. Chen, X.-P. Tian, Y.-T. Shen, and M. Ouhyoung. On visual similarity based 3d model retrieval. In *Computer graphics forum*, volume 22, pages 223–232. Wiley Online Library, 2003. [2](#)
- [5] M. Cimpoi, S. Maji, I. Kokkinos, S. Mohamed, and A. Vedaldi. Describing textures in the wild. In *Proceedings of the IEEE Conference on Computer Vision and Pattern Recognition*, pages 3606–3613, 2014. [2](#)
- [6] J. Deng, W. Dong, R. Socher, L.-J. Li, K. Li, and L. Fei-Fei. Imagenet: A large-scale hierarchical image database. In *Computer Vision and Pattern Recognition, 2009. CVPR 2009. IEEE Conference on*, pages 248–255. IEEE, 2009. [2](#)

[7] J. Donahue, Y. Jia, O. Vinyals, J. Hoffman, N. Zhang, E. Tseng, and T. Darrell. Decaf: A deep convolutional activation feature for generic visual recognition. In *ICML*, pages 647–655, 2014. 2

[8] R. Girshick, J. Donahue, T. Darrell, and J. Malik. Rich feature hierarchies for accurate object detection and semantic segmentation. In *Proceedings of the IEEE conference on computer vision and pattern recognition*, pages 580–587, 2014. 2

[9] X. Han, T. Leung, Y. Jia, R. Sukthankar, and A. C. Berg. Matchnet: Unifying feature and metric learning for patch-based matching. In *Proceedings of the IEEE Conference on Computer Vision and Pattern Recognition*, pages 3279–3286, 2015. 2

[10] K. He, X. Zhang, S. Ren, and J. Sun. Deep residual learning for image recognition. In *Proceedings of the IEEE conference on computer vision and pattern recognition*, pages 770–778, 2016. 7

[11] B. K. P. Horn. Extended gaussian images. *Proceedings of the IEEE*, 72(12):1671–1686, 1984. 2

[12] B.-S. Hua, Q.-H. Pham, D. T. Nguyen, M.-K. Tran, L.-F. Yu, and S.-K. Yeung. Scenenn: A scene meshes dataset with annotations. In *International Conference on 3D Vision (3DV)*, 2016. 4, 5

[13] B.-S. Hua, Q.-T. Truong, M.-K. Tran, Q.-H. Pham, A. Kanezaki, T. Lee, H. Chiang, W. Hsu, B. Li, Y. Lu, et al. Shrec17: Rgb-d to cad retrieval with objectnn dataset. 5, 6

[14] M. Kazhdan, T. Funkhouser, and S. Rusinkiewicz. Rotation invariant spherical harmonic representation of 3 d shape descriptors. In *Symposium on geometry processing*, volume 6, pages 156–164, 2003. 2

[15] G. Klambauer, T. Unterthiner, A. Mayr, and S. Hochreiter. Self-normalizing neural networks. *arXiv preprint arXiv:1706.02515*, 2017. 4

[16] R. Klokov and V. Lempitsky. Escape from cells: Deep kd-networks for the recognition of 3d point cloud models. 2017. 2

[17] Y. LeCun, L. Bottou, Y. Bengio, and P. Haffner. Gradient-based learning applied to document recognition. *Proceedings of the IEEE*, 86(11):2278–2324, 1998. 2

[18] J. Long, E. Shelhamer, and T. Darrell. Fully convolutional networks for semantic segmentation. 2015. 2

[19] D. Maturana and S. Scherer. VoxNet: A 3D Convolutional Neural Network for Real-Time Object Recognition. In *IROS*, 2015. 2, 3, 4, 5, 6

[20] J. McCormac, A. Handa, A. Davison, and S. Leutenegger. Semanticfusion: Dense 3d semantic mapping with convolutional neural networks. *arXiv preprint arXiv:1609.05130*, 2016. 3

[21] G. M. Morton. *A computer oriented geodetic data base and a new technique in file sequencing*. International Business Machines Company New York, 1966. 4, 7

[22] R. A. Newcombe, S. Izadi, O. Hilliges, D. Molyneaux, D. Kim, A. J. Davison, P. Kohli, J. Shotton, S. Hodges, and A. Fitzgibbon. Kinectfusion: Real-time dense surface mapping and tracking. In *The IEEE International Symposium on Mixed and Augmented Reality (ISMAR)*, 2011. 3

[23] M. Nießner, M. Zollhöfer, S. Izadi, and M. Stamminger. Real-time 3d reconstruction at scale using voxel hashing. *ACM Transactions on Graphics (TOG)*, 2013. 3

[24] R. Osada, T. Funkhouser, B. Chazelle, and D. Dobkin. Shape distributions. *ACM Transactions on Graphics (TOG)*, 21(4):807–832, 2002. 2

[25] C. R. Qi, H. Su, K. Mo, and L. J. Guibas. Pointnet: Deep learning on point sets for 3d classification and segmentation. *Proc. Computer Vision and Pattern Recognition (CVPR), IEEE*, 2017. 2, 3, 4, 5, 6, 8

[26] C. R. Qi, H. Su, M. Niessner, A. Dai, M. Yan, and L. J. Guibas. Volumetric and multi-view cnns for object classification on 3d data. In *The IEEE Conference on Computer Vision and Pattern Recognition (CVPR)*, June 2016. 2, 6

[27] C. R. Qi, L. Yi, H. Su, and L. J. Guibas. Pointnet++: Deep hierarchical feature learning on point sets in a metric space. *arXiv preprint arXiv:1706.02413*, 2017. 5, 6

[28] G. Riegler, A. O. Ulusoy, and A. Geiger. Octnet: Learning deep 3d representations at high resolutions. In *Proceedings of the IEEE Conference on Computer Vision and Pattern Recognition*, 2017. 3

[29] A. Sharif Razavian, H. Azizpour, J. Sullivan, and S. Carlsson. Cnn features off-the-shelf: an astounding baseline for recognition. In *Proceedings of the IEEE Conference on Computer Vision and Pattern Recognition Workshops*, pages 806–813, 2014. 2

[30] B. Shi, S. Bai, Z. Zhou, and X. Bai. Deeppano: Deep panoramic representation for 3-d shape recognition. *Signal Processing Letters, IEEE*, 22(12):2339–2343, 2015. 2

[31] N. Silberman, D. Hoiem, P. Kohli, and R. Fergus. Indoor segmentation and support inference from rgbd images. 2012. 2, 4

[32] S. Song, F. Yu, A. Zeng, A. X. Chang, M. Savva, and T. Funkhouser. Semantic scene completion from a single depth image. *Proceedings of 30th IEEE Conference on Computer Vision and Pattern Recognition*, 2017. 3

[33] H. Su, S. Maji, E. Kalogerakis, and E. G. Learned-Miller. Multi-view convolutional neural networks for 3d shape recognition. In *The IEEE International Conference on Computer Vision (ICCV)*, 2015. 2

[34] J. Sun, M. Ovsjanikov, and L. Guibas. A concise and provably informative multi-scale signature based on heat diffusion. In *Computer graphics forum*, volume 28, pages 1383–1392. Wiley Online Library, 2009. 2

[35] D. Thanh Nguyen, B.-S. Hua, L.-F. Yu, and S.-K. Yeung. A robust 3d-2d interactive tool for scene segmentation and annotation. *IEEE Transactions on Visualization and Computer Graphics (TVCG)*, 2017. 3

[36] J. Valentin, V. Vineet, M.-M. Cheng, D. Kim, J. Shotton, P. Kohli, M. Nießner, A. Criminisi, S. Izadi, and P. Torr. Semanticpaint: Interactive 3d labeling and learning at your fingertips. *ACM Trans. Gr.*, 2015. 3

[37] Z. Wu, S. Song, A. Khosla, X. Tang, and J. Xiao. 3d shapenets: A deep representation for volumetric shapes. In *Computer Vision and Pattern Recognition*, 2015. 2, 5, 6

[38] F. Yu and V. Koltun. Multi-scale context aggregation by dilated convolutions. In *ICLR*, 2016. 3